Multiple-scattering contribution in extended X-ray absorption fine structure for iridium oxide IrO_2

1995 J. Phys.: Condens. Matter 7 8027

(http://iopscience.iop.org/0953-8984/7/41/011)

J. Phys.: Condens. Matter 7 (1995) 8027–8033. Printed in the UK

Multiple-scattering contribution in extended x-ray absorption fine structure for iridium oxide IrO_2

E Prouzet

Laboratoire de Chimie des Solides IMN (CNRS UMR110), 2 rue de la Houssinière, 44072 Nantes Cédex 03, France

Received 21 April 1995

Abstract. The influence of multiple-scattering contributions in the x-ray absorption fine structure (XAFS) above the iridium L_{III} edge is discussed for the iridium oxide IrO_2. It is shown that multiple scattering in the IrO_6 cluster cannot explain the occurrence of some features, as previously proposed by comparing with rhenium and tungsten oxide studies. Both the accurate recording of spectra and theoretical calculations lead us to propose that these previously observed features occur from poor signal extraction, especially if the iridium backscattering amplitude is truncated.

1. Introduction

It is now well known that multiple scattering may contribute significantly to x-ray absorption fine structure (XAFS) in a way that prevents analysis of spectra, especially the outer shells, through the classical single-scattering description [1]. For some cases, it can change the EXAFS part (extended x-ray absorption fine structure) in a way that will induce new peaks in the radial distribution function (RDF) around the absorbing atom, which is obtained by Fourier transformation of the EXAFS spectrum. Very clear examples have been recently demonstrated with perovskite type compounds such as tungsten oxides [2] and rhenium oxides [3], and expanded to various structures based on MO_4 or MO_6 clusters [4]. However, it was claimed that for rutile type iridium oxide, IrO_2, a peak appearing at 2.2–3.2 Å between the first oxygen shell and the next iridium shells, in the RDF, was related to the same phenomenon [5, 6]. Indeed, no single-scattering pathway can explain the existence of this peak. Therefore we undertook to check whether this feature in the EXAFS spectrum could be indicative of a multiple-scattering contribution as for perovskite compounds ReO_3 and WO_3, or whether it had to be assigned to another mechanism.

2. Experimental details

X-ray absorption spectra were recorded at the Laboratoire d'Utilisation du Rayonnement Synchrotron (LURE, France), on the DCI ring using 1.85 GeV positrons with an average intensity of 250 mA. They were collected at room temperature in transmission mode at the iridium L_{III} edge ($\approx$ 11 210 eV), on the EXAFS I spectrometer. The monochromator was a Si(331) channel cut and the flux before and after the sample was measured by partially argon filled ionization chambers. The EXAFS spectra were recorded from 11 100 to 12 700 eV with a 3 eV step (2 s time counting). The EXAFS extraction was performed by following the

0953-8984/95/418027+07$19.50

standard procedure [7] using software written by Michalowicz [8]. The EXAFS contribution of the absorption spectrum can be written as

$$\chi(E) = \frac{\mu(E) - \mu_1(E)}{\mu_1(E) - \mu_0(E)} \tag{1}$$

where $\mu(E)$ is the observed signal, $\mu_1(E)$ the single atomic absorption of the absorber and $\mu_0(E)$ the background absorption that the sample would undergo in the same energy range without any absorption edge jump. This signal is usually described in the k space, where k is the wave vector in Å^{-1} and is related to the energy E in eV through the relation

$$k = \sqrt{\frac{2m_e(E - E_0)}{\hbar^2}} \tag{2}$$

with m_e the electron mass, h the Planck constant and E_0 the energy of the absorption edge. $\mu_0(E)$ is calculated by using a theoretical expression developed by Lengeler and Eisenberger [9]; $\mu_1(E)$ is interpolated by a fifth-degree polynomial between 11 220 eV and 12 700 eV. The E_0 value is set at the half jump in the edge, equal to 11 210 eV. The pseudo-radial distribution function (RDF) is then obtained by a Fourier transform of the weighted $\omega(k)k^2\chi(k)$ spectra, where $\omega(k)$ is a weighting window using a Kaiser function ($\tau = 2.5$) defined between 3 and 20 Å^{-1}. The RDFs are uncorrected from atomic phase shift.

The iridium oxide powder was synthesized through a new way of synthesis leading first to an amorphous iridium oxihydroxide then to a well crystallized iridium oxide powder [10, 11]. The latter presents a crystalline framework that exhibits no distortion from the expected quadratic $P4_2/mnm$ symmetry, in contrast to that observed for commercial provided powders [6, 11]. The powder was ground to 20 μm, then deposited on a Kapton™ adhesive film.

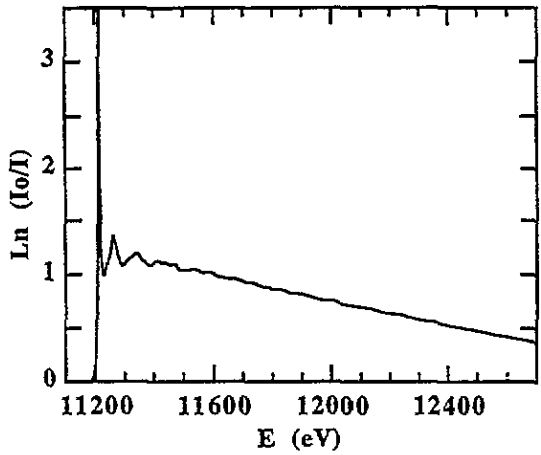

Figure 1. Experimental absorption spectrum at the iridium L_{III} edge for the iridium oxide IrO_2.

Theoretical spectra were obtained from the fast multiple-scattering calculation developed by Rehr (FEFF-5 code) [12, 13]. This approach can be summarized as below. From the crystallographic data, an atomic potential is built in a sphere around the absorbing atom. The atomic phases are calculated and all the possible paths of the photoelectron ejected from the absorbing atom, and going back to it, are then found. A first scattering calculation with a plane wave formalism gives quickly the relative weights of each pathway in the

absorbing cross-section. Once the less contributing pathways have been removed, a second calculation with a curve wave formalism is thus performed and the EXAFS contribution can be deduced for each pathway. We did not take into account the Debye–Waller parameter.

3. Results and discussion

The raw absorption spectrum and EXAFS spectrum of IrO_2 are displayed in figures 1 and 2, respectively. The EXAFS spectrum exhibits a signal up to 20 $Å^{-1}$, due to the backscattering amplitude of iridium neighbours. The modulus of the Fourier transform of this EXAFS spectrum is given in figure 3. It is characterized by a first peak (peak 1) at 1.5 Å, due to the oxygen backscatterers in the first shell around iridium. One can identify a group of three peaks (peaks 2, 3 and 4) between 2.5 and 4.0 Å, one at 4.5 Å (peak 5) and another at 5.5 Å (peak 6). Other peaks can be also seen after 6.0 Å. The RDF of the amorphous iridium oxihydroxide is also given for comparison [10, 11]. For both curves, we do not observe any peak between 2.0 and 3.0 Å, except the small peak 2. These spectra show that the additional contribution previously reported to peak in this distance range is not always observed.

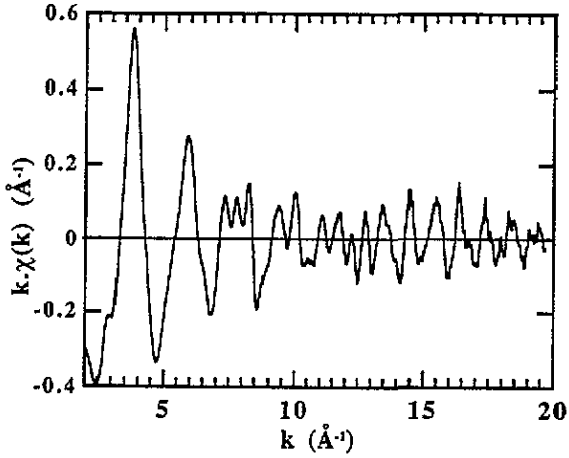

Figure 2. Experimental XAFS spectrum $k\chi(k)$ at the iridium L_{III} edge for the iridium oxide IrO_2, obtained from the spectrum shown in figure 1.

The theoretical EXAFS spectrum of IrO_2 was calculated by starting from the crystallographic positions given in table 1 [6], and by including all the scattering paths in a 7 Å radius sphere surrounding an iridium atom. The first ones are given in table 2. Paths I and II are single scattering in the IrO_6 cluster. The next shortest pathway (III) is also a single-scattering path with the closest iridium at 3.155 Å as backscatterer. The path IV is double scattering in the IrO_6 cluster. By comparison with other compounds [2–4], this path should induce the additional peak. The EXAFS spectrum resulting from all scattering paths is exhibited in figure 4. One can see that all the features of the experimental EXAFS spectrum are well reproduced by this calculation, even if, as we did not take into account the Debye–Waller parameter, the intensities cannot be compared, especially at high k. This shows that our calculation using FEFF is meaningful and that we can use it to analyse the single contribution of each scattering path. The EXAFS contribution for the pathway IV is also presented. Its intensity is weak and it gives a significant contribution only below 8 $Å^{-1}$.

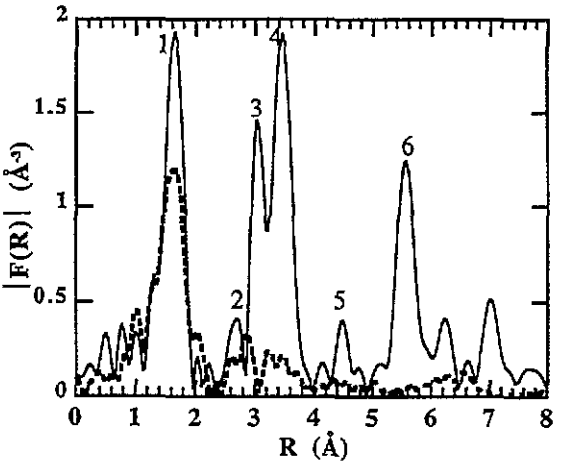

Figure 3. Modulus of the Fourier transform of $k^2\chi(k)$ spectra at the iridium L_{III} edge for the iridium oxide IrO_2 (solid line) and for an amorphous iridium oxihydroxide (dashed line). The numbers refer to the text.

Table 1. Atomic positions for the iridium oxide IrO_2. The cell symmetry is $P4_2/mnm$ with parameters $a = b =$ 4.4983(1) Å and $c = 3.1547(2)$ Å.

Position	Atom	x	y	z
1(a)	Ir	0	0	0
2(f)	O	0.308(2)	0.308(2)	0

Table 2. First scattering paths used in calculations of the Ir L_{III} edge absorption spectrum. The absorbing atom is indicated by *, the length is the effective length of the photoelectron path and amplitudes are relative values.

	Pathway	Degeneracy	Length ( )	Amplitude
I	Ir*–O–Ir*	2	3.918	100
II	Ir*–O–Ir*	4	3.990	100
III	Ir*–Ir–Ir*	2	6.310	19.3
IV	Ir*–O–O–Ir*	16	6.750	24.7
V	Ir*–O–Ir*	4	6.814	25.0
VI	Ir*–Ir–Ir*	8	7.100	60.1
VII	Ir*–O–O–Ir*	4	7.144	5.5
VIII	Ir*–Ir–O–Ir*	4	7.428	19.5
IX	Ir*–O–Ir*	8	7.504	8.6
X	Ir*–Ir–O–Ir*	8	7.504	8.6
XI	Ir*–Ir–O–Ir*	2	7.838	6.3
XII	Ir*–O–O–Ir*	2	7.838	17.7

Figure 5 compares the experimental RDF to RDFs obtained from different scattering pathways. If we compare it first to the RDF obtained with single-scattering paths only, we see that single scattering allows us to explain quite well all the contributions below 3.6 Å. The peak 2, especially, that could be linked to the double scattering (pathway IV), is well reproduced by only single scattering. The RDF of the contribution of pathway IV is given also in figure 5. It is obvious that if it peaks at the expected distance, it is very diffuse and

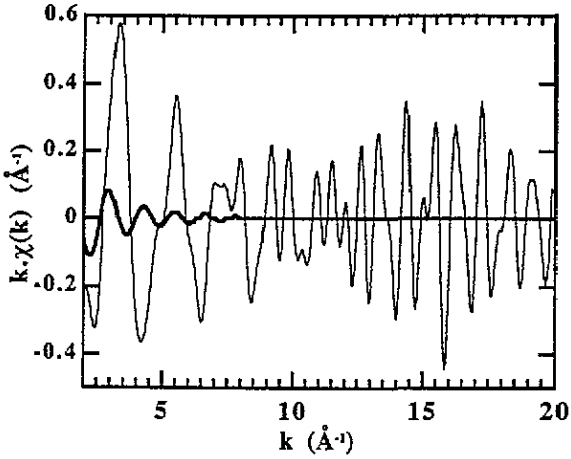

Figure 4. Calculated XAFS spectrum $k\chi(k)$ at the iridium L_{III} edge for the iridium oxide IrO_2 (thin line) and the scattering contribution corresponding to pathway IV (bold line).

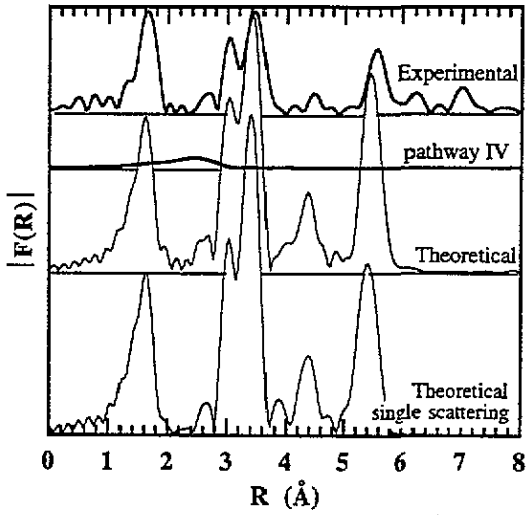

Figure 5. Modulus of the Fourier transform of $k^2\chi(k)$ spectra at the iridium L_{III} edge for (top to bottom) the experimental IrO_2 spectrum, the pathway IV contribution, the calculated IrO_2 spectrum and a calculated spectrum including only the single-scattering contributions.

its intensity cannot explain any kind of significant peak in this region, in contrast to what was observed for ReO_3 or WO_3 for instance [2–4].

In order to determine precisely the weight of the multiple-scattering contribution, we report in figure 6 the imaginary parts and modulus of the Fourier transform of EXAFS spectra calculated with whole-scattering or only single-scattering contributions. The difference between them was obtained by subtracting the imaginary parts. It leads to the multiple-scattering contribution, which is also reported. One can see that the peaks 1, 2, 3 and 5 are only due to single scattering whereas the peak 4 contains a small fraction of multiple scattering. This fraction interferes with the single-scattering part and the intensity of the resultant signal is weaker than for single scattering alone. Such an interference is well seen for the peak 6. Indeed, for this peak, both single and multiple scattering have the same

intensity. Nevertheless, as they are not in phase, the addition of the two imaginary parts—so the whole scattering spectrum—does lead to a contribution with almost the same intensity but not the same frequency. The related EXAFS contribution cannot thus be linked to any real distance through the classical formalism [1]. This example shows also how it may be dangerous to compare only the modulus of the Fourier transform in order to explain the relative parts of each scattering path.

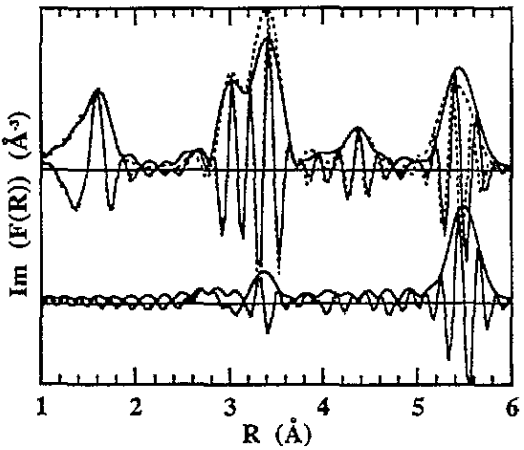

Figure 6. Top, modulus and imaginary part of the Fourier transform of $k^2\chi(k)$ spectra at the iridium L_{III} edge for the calculated spectrum including all the scattering contributions (solid line) and a calculated spectrum including only the single-scattering contributions (dashed line). Bottom, Modulus and imaginary part of the Fourier transform of $k^2\chi(k)$ spectra including only the multiple-scattering contributions.

These results show that, first, one can obtain an EXAFS spectrum of iridium oxide that does not exhibit the additional peak previously reported, and, second, that multiple-scattering contributions cannot explain the hypothetical existence of such a peak. Therefore we decided to check whether the EXAFS analysis procedure could explain the previous results. Figure 7 exhibits RDFs obtained from the same EXAFS spectrum (figure 2) with different weighting windows $\omega(k)$ equal to 3–9 $Å^{-1}$, 3–13 $Å^{-1}$, 3–15 $Å^{-1}$ and 3–19.6 $Å^{-1}$ for figures 7(a), (b), (c), (d) respectively. Iridium is a heavy atom and its backscattering amplitude extends up to 20 $Å^{-1}$, as can be seen in figure 3. So, taking a too short weighting window—or recording spectra in a too short energy range—will lead to a truncation of this amplitude and will disturb the resultant signal. This is confirmed in figure 7(a) and (b) for which a significant contribution is observed in the 2.2–3.2 Å range, which is the range previously reported to exhibit an additional peak [5, 6]. As the weighting window increases, this contribution decreases. If it is still observed for the 3–15 $Å^{-1}$ window (figure 7(c)), the Fourier transform on the whole energy range leads to its extinction. We may recall that the RDF of the iridium oxihydroxide EXAFS spectrum (figure 3), recorded with the same conditions, does not exhibit also any suspect peak.

4. Summary and conclusions

We have presented a study reporting some multiple-scattering contributions in the iridium oxide IrO_2. *We have shown that some contributions that had been reported in previous* works [5, 6], cannot be attributed to multiple-scattering phenomena as has been shown for

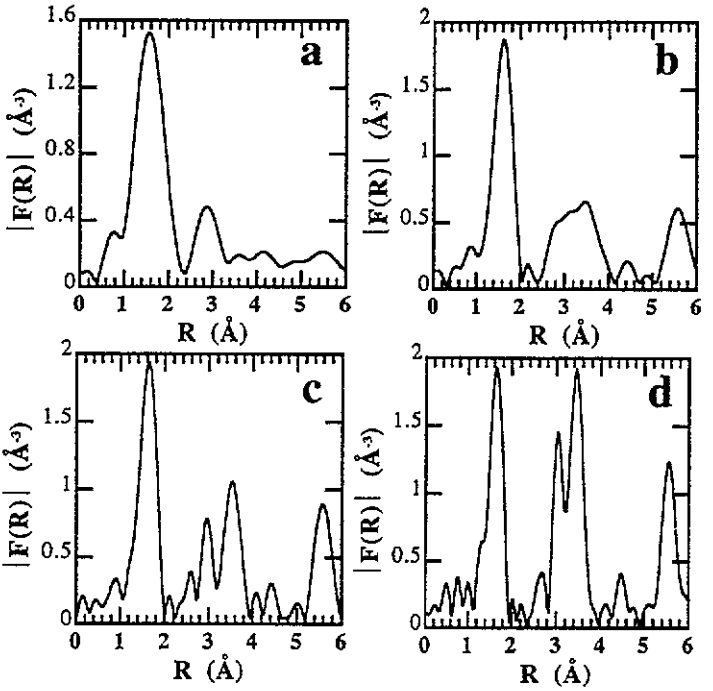

Figure 7. Comparison of the RDFs obtained from the experimental spectrum shown in figure 2, by varying the range of the weighting window $\omega(k)$. (a) 3–9 $Å^{-1}$, (b) 3–13 $Å^{-1}$, (c) 3–15 $Å^{-1}$, (d) 3–19.6 $Å^{-1}$.

other compounds [2–4]. An accurate recording of data in a long enough energy range (i.e. 1500 eV after the iridium L_{III} edge) leads to spectra that do not exhibit these features, if the EXAFS analysis—and mainly the weighting window in the Fourier transform—takes into account the information in this whole range of energy.

Acknowledgment

The author thanks P Moreau for help in multiple-scattering calculations.

References

[1] Lyttle F W, Sayers D E and Stern E A 1975 *Phys. Rev.* B **11** 4825
[2] Kuzmin A and Purans J 1993 *J. Phys.: Condens. Matter* **5** 9423
[3] Kuzmin A, Purans J, Benfatto M and Natoli C R 1993 *Phys. Rev.* B **47** 2480
[4] Kuzmin A and Grisenti R 1994 *Phil. Mag.* B **70** 1161
[5] Balerna A, Bernieri E, Burattini E, Kuzmin A, Lusis A, Purans J and Cikmach P 1991 *Nucl. Instrum. Methods Phys. Res.* A **308** 234
[6] Bestaoui N, Prouzet E, Deniard P and Brec R 1993 *Thin Solid Films* **235** 35
[7] Teo B K 1986 *EXAFS: Basic Principles and Data Analysis* (Berlin: Springer)
[8] Michalowicz A1991 *Logiciels pour la Chimie* (Paris: Société Française de Chimie)
[9] Lengeler B and Eisenberger P 1980 *Phys. Rev.* B **21** 4507
[10] Bestaoui N and Prouzet E 1994 Patent FR 94/06773
[11] Bestaoui N and Prouzet E submitted
[12] Rehr J J, Zabintski S I and Albers R C 1992 *Phys. Rev. Lett.* **69** 3397
[13] Rehr J J 1993 *Japan. J. Appl. Phys.* **32** 8